

# The 42<sup>nd</sup> Annual BIO481Y5 Symposium

April 12, 2021  
9:00 am to 4:30pm



## BIO481 – April 12, 2021 – Abstracts and Presentations

### Session I – 9:15 am to 12:15 pm – Moderator: Peter Kotanen

9:15 am	<a href="#"><u>Riya Philip (Angela Lange)</u></a>
9:30 am	<a href="#"><u>Faraz Quershi (Angela Lange)</u></a>
9:45 am	<a href="#"><u>Syed Hassan Rizvi (Angela Lange)</u></a>
10:00 am	<a href="#"><u>Lina Alsaghir (Angela Lange)</u></a>
10:15 am	<a href="#"><u>Haya Habib (Ted Erclik)</u></a>
<b>10:30 am</b>	<b>Coffee Break</b>
10:45 am	<a href="#"><u>Osama Abdalla (Joel Levine)</u></a>
11:00 am	<a href="#"><u>Alyssa Ialongo (Ho Sung Rhee)</u></a>
11:15 am	<a href="#"><u>Sarah De Costa (Tim Westwood)</u></a>
11:30 am	<a href="#"><u>Maria Roussi (Tim Westwood)</u></a>
11:45 am	<a href="#"><u>Erla Hidi (Tim Westwood)</u></a>
12:00 pm	<a href="#"><u>John Stone (Tim Westwood)</u></a>

### Session II – 1:00 pm to 4:15pm – Moderator: Peter Kotanen

1:00 pm	<a href="#"><u>Yeshoda Harry-Paul (Rob Ness)</u></a>
1:15 pm	<a href="#"><u>Wen Tong (Alex Nguyen Ba &amp; Rob Ness)</u></a>
1:30 pm	<a href="#"><u>Stephanie Shishis (Robert Gerlai)</u></a>
1:45 pm	<a href="#"><u>Joshua Hung (Marcus Dillon)</u></a>
2:00 pm	<a href="#"><u>Marian Saab (Melissa Holmes)</u></a>
2:15 pm	<a href="#"><u>Fiona Ramnarain (Brandon Walters)</u></a>
<b>2:30 pm</b>	<b>Break</b>
2:45 pm	<a href="#"><u>Deryk Vu (Steven Short)</u></a>
3:00 pm	<a href="#"><u>Erin Beauchesne (Robert Reisz)</u></a>
3:15 pm	<a href="#"><u>Sofia Pereira (Bailey McMeans)</u></a>
3:30 pm	<a href="#"><u>Wanzhang Wang (Mary Cheng)</u></a>
3:45 pm	<a href="#"><u>Lingfeng Ma (Mary Cheng)</u></a>
4:00 pm	<a href="#"><u>Saumya Mathur (David McMillen)</u></a>

The Effect of Gonadulin on *Rhodnius Prolixus* Reproduction

Insulin-like peptides (ILPs) are vital hormones involved in a wide range of physiological processes in arthropods. They are sensors of positive nutritional state and regulators of many anabolic processes in adult insects. The triatomine, *Rhodnius prolixus*, is a blood-feeding insect, and one of the main vectors of an inflammatory condition, Chagas disease, prevalent in the South and Central Americas. The blood meal has a high epidemiological impact as it initiates egg development, leading to laying batches of eggs. Based on publicly available transcriptomes, a new ILP named gonadulin, was found to be orthologous to *Drosophila* ILP8, and suggested to be expressed by the gonads in *R. prolixus*. To understand its role during egg-laying, transcript levels of gonadulin and a dILP8-receptor ortholog, LGR3, were analysed from various tissues of adult female insects in fed and unfed conditions. The spatial and temporal mRNA distribution showed greatest gonadulin and LGR3 expression in the ovaries and fat bodies, respectively in the unfed condition (Figures 1 and 2). Transcript knockdown of gonadulin, using double-stranded RNA, resulted in a downregulation of the main yolk protein precursor, vitellogenin, in the fat body (Figure 3). These results show that the signalling between ovaries and fat bodies is enhanced with prolonged starvation and appears to be involved in the regulation of vitellogenesis, i.e., synthesis of yolk protein in fat body and uptake by the oocyte. Understanding the molecular mechanisms of *R. prolixus*' reproductive performance can shed light on potential targets for effective synthesis of biopesticides, thereby controlling the *R. prolixus* population and transmission of the disease.

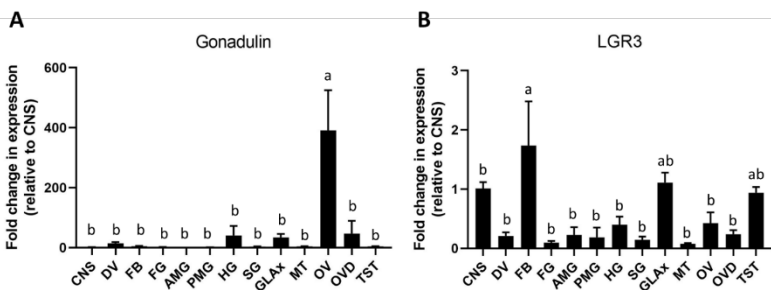


**Figure 1: Spatial distributions of gonadulin and its receptor (LGR3) transcripts in various tissues of *R. prolixus*.** Unfed females were dissected 10 days post-ecdysis, and tissues were separated into 14 groups: Central nervous system (CNS), dorsal vessel (DV), fat body (FB), foregut (FG), anterior midgut (AMG), posterior midgut (PMG), hindgut (HG), salivary glands (SG), accessory glands (GLAx), hemocyte (HE), Malpighian tubules (MT), ovaries (OV), oviduct (OVD), testes (TST). Transcript levels of gonadulin (A) and LGR3 (B) were quantified using RT-qPCR and the  $\Delta\Delta C_t$  method. The y-axis represents the fold change in expression relative to CNS (value ~ 1) obtained via geometric averaging using 18S and actin rRNA as reference genes. The results are shown as mean  $\pm$  SEM of 3-5 independent experiments. Statistical analysis was performed using a one-way ANOVA and Tukey's test for post-hoc analysis. Significant of  $P < 0.05$  is denoted using letters to indicate bars that are significantly different from others.

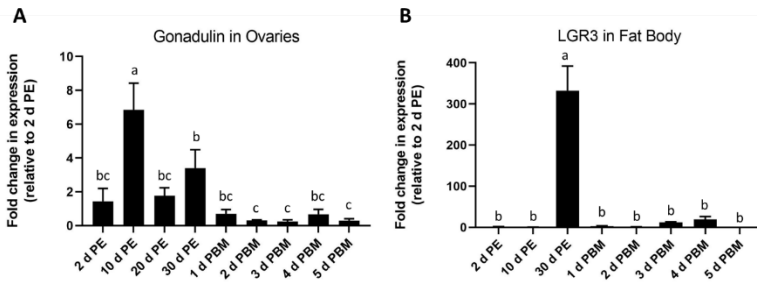


**Figure 2: Temporal expression levels of gonadulin and LGR3 transcript in *R. prolixus* females.** Unfed females were dissected 2, 10, 15, 20, and 30d PE to analyze the unfed condition. A separate group was fed, and respective tissues were dissected at 1,2,3,4, and 5 days post-blood meal (d PBM) to analyze the fed conditions. Expression levels of gonadulin in ovaries (A) and LGR3 in fat bodies (B) were quantified using RT-qPCR and the  $\Delta\Delta C_t$  method. The y-axis represents the fold change in expression relative to 2d PE (value ~ 1) obtained using 18S rRNA as the reference gene. The results are shown as mean  $\pm$  SEM of 3-5 independent experiments. Statistical analysis was performed using a one-way ANOVA and Tukey's test for post-hoc analysis. Significant of  $P < 0.05$  is denoted using letters to indicate bars that are significantly different from others.

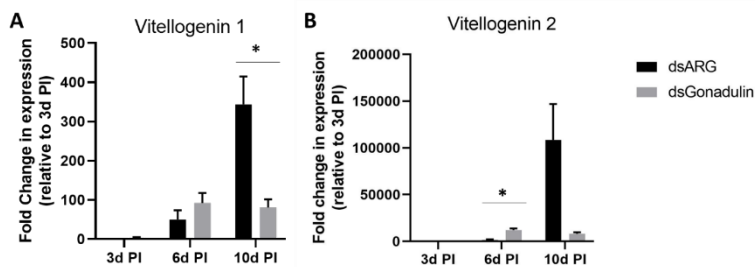


**Figure 3: Effect of dsRNA injection to knockdown gonadulin transcript levels on vitellogenin expression in fat body.** RT-qPCR assays were performed on fat bodies to analyze (A) *vitellogenin 1* and (B) *vitellogenin 2* transcript expression in females at 3-, 6-, and 10-days post-injection (d PI) with dsGonadulin. The y axis represents the fold change in expression relative to 3d PI of the respective group (value ~ 1) obtained using 18S rRNA as reference gene. The results are shown as mean  $\pm$  SEM of 5 independent experiments. The statistically significant difference was inferred using nonparametric t-tests. Significant of  $P < 0.05$  is denoted using asterisks to indicate significant difference from control.

Dissecting the Role of Serotonin Signaling in *Rhodnius Prolixus* Reproduction

Serotonin (5-hydroxytryptamine, 5-HT) is a hormone with a variety of functions in both insects and humans. In the blood-gorging insect, *Rhodnius prolixus*, it acts as a diuretic hormone. Since it plays a role in oviposition in beetles, it was hypothesized that it might play a similar role in *R. prolixus*. This insect is anautogenous and therefore needs a blood meal to produce eggs. To date, there are five serotonin receptors identified in insects: 5-HT1A, 5-HT1B, 5-HT2A, 5-HT2B and 5-HT7. It was found that the 5-HT7 had the highest transcript expression. Furthermore, 5-HT7 expression in oviducts increased over time and was higher in the fed condition compared to the unfed condition. The presence of serotonin receptor in the oviducts indicates that it might play a role in reproduction in *R. prolixus*. An egg-laying assay was performed to see if serotonin alters oviposition. Insects were injected with serotonin (treatment, n=10) or physiological saline (control, n=10) 4d post blood meal (PBM). The percent of egg-laying insects was 90% in the control group and 70% in the treatment group, with the control group laying 9.7 eggs/insect while the treatment group laid 7.6 eggs/insect. Interestingly, 7 eggs in the treatment group were white. Previous studies have shown that eggs of *R. prolixus* are pink-colored due to a heme-binding protein that is necessary for embryo development. The current study suggests that serotonin may play a role in ovulation but also in egg development. However, further studies are needed to determine the precise role of serotonin in reproduction.

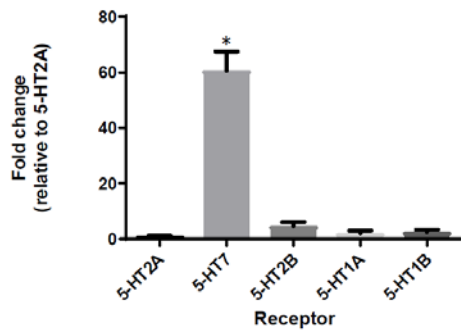


Figure 2 Expression of 5-HT receptor transcripts in *R. prolixus* oviducts at 5d PBM. Data are mean ± SEM for n=6. Statistical analysis was done using one-way ANOVA and Tukey's test for post-hoc analysis. \* p<0.05 vs 5-HT2A, 5-HT2B, 5-HT1A, 5-HT1B

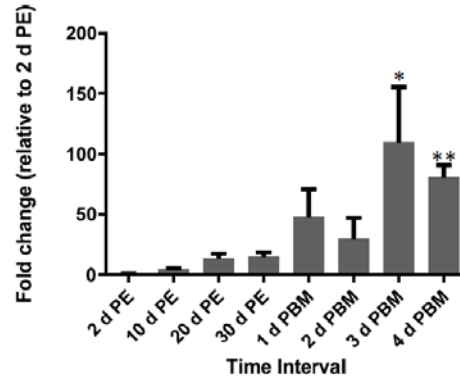
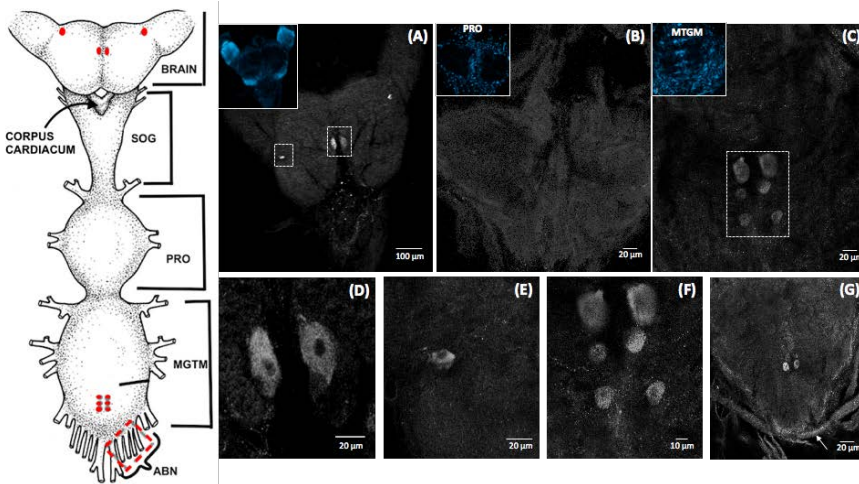


Figure 1 Temporal expression of 5-HT7 receptor transcript in *R. prolixus* oviducts in unfed and fed condition (days post blood meal, PBM). Data are mean ± SEM for n=3-6. Statistical analysis was done using one-way ANOVA and Tukey's test for post-hoc analysis. \* p<0.05 vs 2, 10, 20, 30dPE; 1, 2d PBM. \*\* p<0.05 vs 4d PE; 1,2d PBM.

Analyzing the effect of Octopamine, a biogenic amine, on the Egg Laying of *Rhodnius prolixus*

*Rhodnius prolixus* is a blood-feeding insect that requires a blood-meal for development and reproduction. *R. prolixus* is a vector for the parasite *Trypanosoma cruzi*, which is the cause of Chagas disease that affects millions in Central and South America. Octopamine (OA), a biogenic amine, has been known to decrease spontaneous contractions of the oviducts and bursa, tissues involved in reproduction. Here we studied the effect of OA on the reproductive physiology of *R. prolixus*. Using immunofluorescence, I identified neurons in the central nervous system (CNS) with positive signal to tyrosine decarboxylase, an enzyme involved in OA synthesis, along with immunoreactivity in axons indicating possible release sites into the circulation (Fig. 1). By RT-qPCR, I found that after feeding, the expression to tyramine  $\beta$  hydroxylase, the enzyme involved in OA synthesis, increased in CNS, indicating that the blood meal would be a signal to its synthesis. At day 5 post blood-meal, when egg-laying starts, the transcript expression to the octopamine  $\beta$ -adrenergic receptor, *RhoprOct $\beta$ 2-R*, was highest in CNS, followed by tissues involved in contractions, such as oviduct and bursa (Fig. 2). The temporal expression showed an upregulation of *RhoprOct $\beta$ 2-R* mRNA in oviducts after feeding, which supports the hypothesis that OA is important for ovulation. Using RNAi assays to downregulate the *RhoprOct $\beta$ 2-R*, the transcript expression to the main yolk protein, vitellogenin, decreased significantly in the fat body, a key player involved in nutrients synthesis. Overall, I suggest that OA/*RhoprOct $\beta$ 2-R* is involved in egg formation and ovulation; however, further experimentation is required.



**Fig 1.** Immunohistochemistry for Tyrosine decarboxylase, TDC, an enzyme in the pathway leading to synthesis of OA in female adult *R. prolixus* CNS. The image on the left is the CNS of *R. prolixus* and labels A-G demonstrate the TDC signaling in the different regions of CNS. (A) TDC-like immunoreactive neurons are found in the brain. (B) No TDC immunoreactive signals were found in the prothoracic ganglion (PRO). (C) Pairs of TDC immunoreactive neurons in mesothoracic ganglionic mass (MTGM). (F) Higher magnification of the OA signaling in MTGM. (D) TDC signaling observed in the middle of the brain with a higher magnification. (E) TDC signaling in the lobes of the brain with a higher magnification. (F) Higher magnification of the TDC signaling in MTGM. (G) Neuronal projections of TDC at the proximal end of MTGM.

**Spatial distribution of *RhoprOct $\beta$ 2-R* (5 d PBM)**

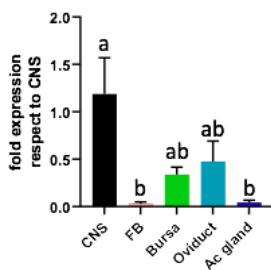


**Fig. 2** The spatial distribution of the transcript expression to the octopamine  $\beta$ -adrenergic receptor, *RhoprOct $\beta$ 2-R* in CNS and other PB tissues involved in reproduction. The spatial distribution is observed in insects day 5 post blood-meal, which is when egg-laying starts. Statistical analysis was performed using a one-way ANOVA and Tukey's test for post-hoc analysis. Significance of  $P < 0.05$  is denoted using letters to indicate bars that are significantly different from others.

Role of serotonin in metabolism pathways in the fat body of *Rhodnius prolixus*, a blood-gorging insect

Serotonin, or 5-Hydroxytryptamine (5-HT), is an amine neurotransmitter with a vital role in animals. 5-HT is examined in relation to metabolism using the experimental organism *Rhodnius prolixus*, a blood-gorging insect. Previous studies found that 5-HT titres increase in the hemolymph (blood) shortly after a blood meal, and this was also suggested here by measuring of two enzymes involved in the biosynthetic pathway that leads serotonin production (Fig. 1). I used fat-body (FB), a tissue involved with general metabolism in insects, to measure the expression of 12 transcripts involved in carbohydrate, lipid, and protein metabolism under physiological conditions. The results showed an increase in the expression for metabolism-related transcripts post-feeding. To assess the direct 5-HT involvement in metabolism, the fed condition was stimulated “artificially” from unfed females using *in-vivo* and *ex-vivo* assays. Overall, the results from these experiments confirmed that 5-HT increases the transcript expression of metabolism-related transcripts (Fig. 2). To confirm that the FB is a main organ targeted by 5-HT, the expression of 5 different 5-HT receptors in the FB was tested; showing that 5HT2A had the highest transcript expression (Fig. 3). 5HT2A transcript expression was also evaluated in other 12 tissues. In conclusion, 5-HT signalling is involved in the metabolism in female *R. prolixus* and might play a role in reproduction given the importance of nutrients in egg development. Future studies are needed to support this hypothesis by knocking down 5HT2A receptor and evaluating both the expression of metabolism-related proteins and egg formation.

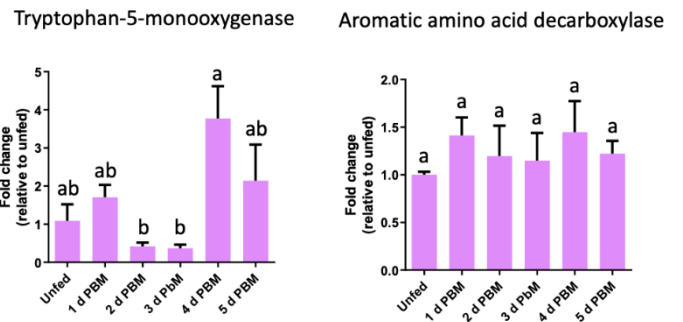


Figure 1: Transcript expression of two enzymes involved in the biosynthetic pathway leading to the production of serotonin in CNS of *Rhodnius prolixus* females over the span of 5 days post blood meal (fed condition). The y-axis represents the fold change in expression relative to unfed condition. The results are shown as mean ± SEM (n=4). Statistical analysis was performed using a one-way ANOVA and Turkey’s test for post-hoc analysis, where different letters indicate significant difference at  $P < 0.05$ .

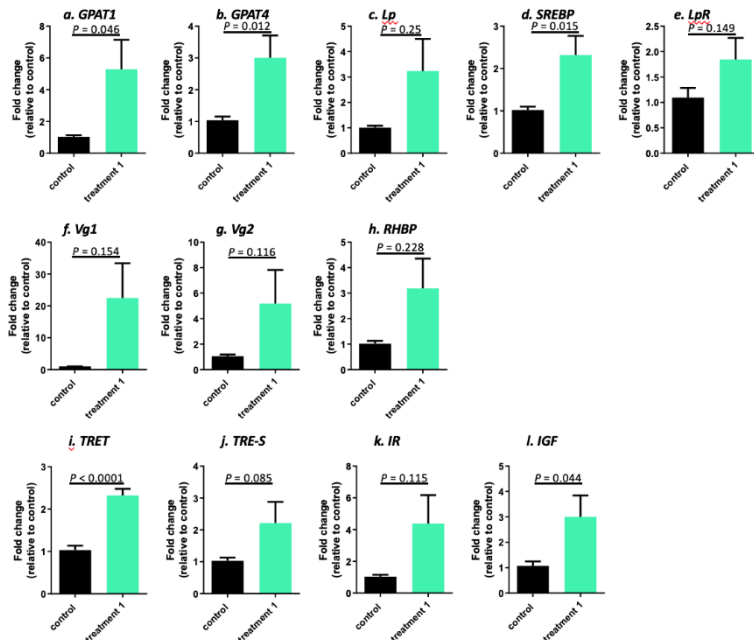


Figure 2: Transcript expression of 12 metabolism-related transcripts in serotonin-stimulated fat body by *in-vivo* assays in *Rhodnius prolixus* females. The treatment group was injected with 5 ul of 4 pmol serotonin concentration and was compared to the control group that was injected with 5 ul saline. a-e) Transcripts related to lipid metabolism, f-h) Transcripts related to protein metabolism, and i-l) Transcripts related to carbohydrate metabolism. The y-axis represents the fold change in expression relative to control. The results are shown as mean ± SEM of n=8, where each n represents an individual tissue from 1 insect. Statistical analysis was performed using Student’s t-test.

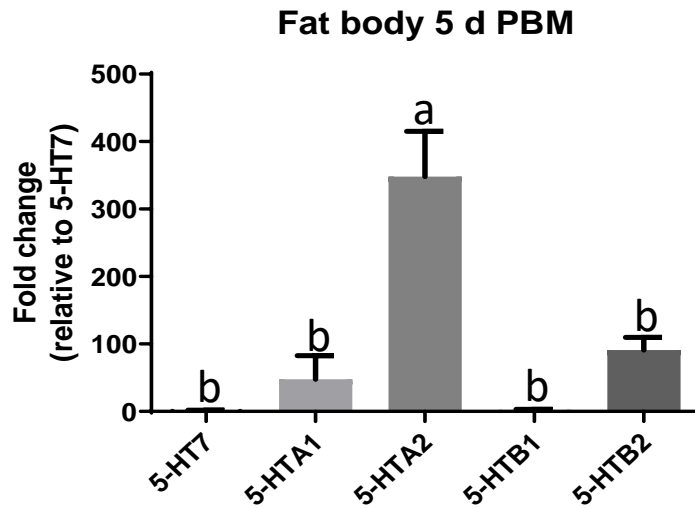


Figure 3: Relative transcript expression of 5 different serotonin receptors in the fat body of female *Rhodnius prolixus*: 5-HT7, 5-HTA1, 5-HTA2, 5-HTB1, and 5-HTB2. The y-axis represents the fold change in expression relative to 5-HT7. The results are shown as mean  $\pm$  SEM (n=4-5). Statistical analysis was performed using a one-way ANOVA and Turkey's test for post-hoc analysis, where different letters indicate significant difference at  $P < 0.05$ . Plot shows that 5-HTA2 has the highest transcript expression relative to 5-HT7.

10:15 am

Haya Habib (Ted Erclik)

Long range temporal patterning of neurogenesis in the *Drosophila* visual system

The *Drosophila* optic lobe is an excellent model system for the study of neural circuit assembly, with thousands of neurons precisely organized into a retinotopic circuit. The medulla is the largest and most diverse structure in the optic lobe, with more than 100 neuronal types. These neurons are generated by neural stem cells, termed neuroblasts, which are continuously specified over a 2-day period in the late larva. Previous work has shown that medulla neuroblasts are patterned spatially and temporally to generate neural diversity. However, to date, it has not been shown whether the timing of a neuroblast's specification can also act as a mechanism to generate diversity. For example, does a neuroblast specified at 70h of larval development generate different neurons than a neuroblast specified at 80h? Here, I show that neuroblasts specified at different times do generate distinct neural types. I used the EdU labelling technique, in which larvae are fed EdU to permanently incorporate this Thymidine analog into neurons born during the feeding window, to determine the birth date of two medulla neurons: Dm6 and Dm12. Remarkably, I found that Dm6 and Dm12 neurons are born in two distinct EdU feeding windows; Dm6 neurons are labelled with EdU between ~68 to 72h whereas Dm12 neurons are labelled between ~72 and 76h. This data suggests that in addition to spatial and temporal patterning mechanisms, the larval age in which a neuroblast is specified acts as a third patterning mechanism to increase neural diversity. Future studies will determine whether this long range temporal patterning mechanism plays a general role in medulla neurogenesis.

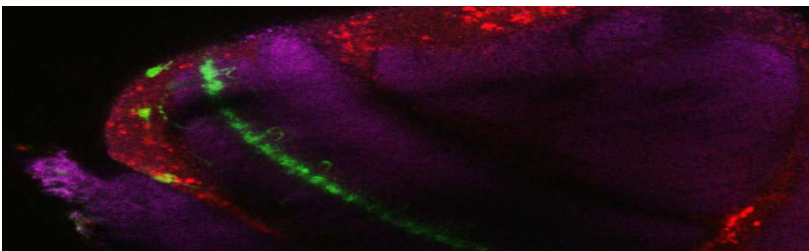
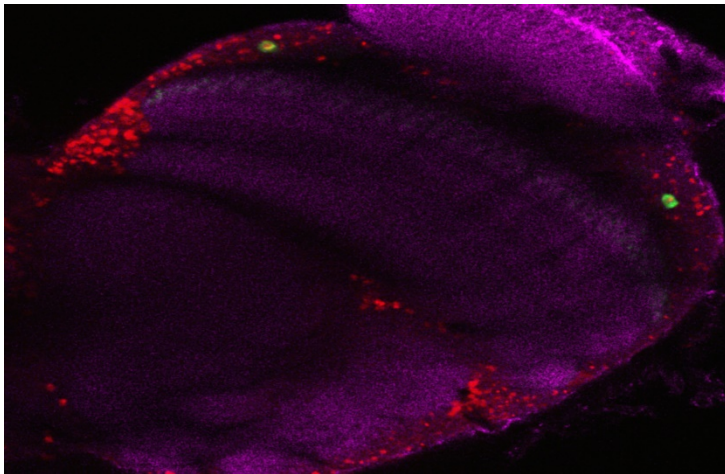


Figure 1: Dm12 neurons labelled with EdU. Green fluorescent protein (GFP) marks the location of the Dm12 cell bodies whereas the red color shows all the EdU labelled cells



**Figure 2:** Dm6 neurons labelled with EdU. Green fluorescent protein (GFP) shows the location of Dm6 cell bodies whereas the red color shows all EdU labelled cells

10:30 am

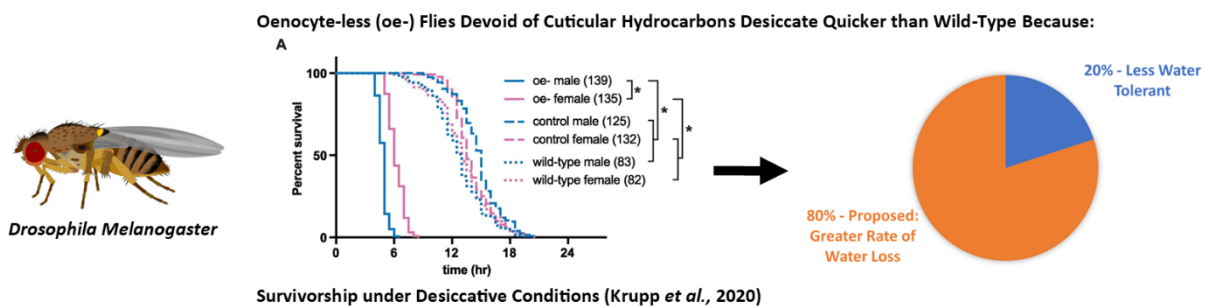
Break

10:45 am

Osama Abdalla (Joel Levine)

### Desiccation Resistance and the Protective Role of Insect Cuticular Hydrocarbon Compounds

Terrestrial organisms have evolved various mechanisms to protect against desiccation. For example, hydrocarbons (HCs) on the surface of the insect cuticle have been implicated in reducing the rate of evaporative water loss<sup>1-3</sup>. A recent study used oenocyte-less flies (oe-), a genetically engineered strain of *Drosophila melanogaster* lacking HCs to determine the role of these compounds in protecting against desiccation<sup>4</sup>. The study found that the survival of oe-flies under desiccation conditions was compromised relative to wild-type controls, and that the lack of HCs was likely responsible for this phenotype. In the current study, we asked: could the decreased survival of oe- flies under desiccation be due to (1) the inability to tolerate water loss; (2) the lack of sufficient internal body water stores; or (3) a greater rate of water loss across the cuticle. It is predicted that oe- flies lose water at a greater rate, and if true, then coating oe- flies with HCs should rescue the rate of water loss phenotype. The 3 questions were addressed using gravimetric methods. Results thus far suggest that decreased water loss tolerance and reduced internal body water storage are minor contributors (5-20% total) to the reduced survival of oe- flies under desiccation conditions. My findings therefore indicate that oe- flies are more susceptible to desiccation due to a greater rate of water loss. These results will add to a growing body of evidence that insect HCs protect against desiccation by reducing the rate of water loss across the cuticle.



## References

- (1) Hadley, N. F.; Machin, J.; Quinlan, M. C. Cricket Cuticle Water Relations: Permeability and Passive Determinants of Cuticular Water Content. *Physiol. Zool.* **1986**, *59* (1), 84–94. <https://doi.org/10.1086/physzool.59.1.30156094>.
- (2) Hadley, N. F.; Quinlan, M. C. Cuticular Permeability of the Black Widow Spider *Latrodectus Hesperus*. *J. Comp. Physiol. B* **1989**, *159* (3), 243–248. <https://doi.org/10.1007/BF00691500>.
- (3) Gibbs, A. G.; Chippindale, A. K.; Rose, M. R. Physiological Mechanisms of Evolved Desiccation Resistance in *Drosophila Melanogaster*. *J. Exp. Biol.* **1997**, *200* (12), 1821 LP – 1832.
- (4) Krupp, J. J.; Nayal, K.; Wong, A.; Millar, J. G.; Levine, J. D. Desiccation Resistance Is an Adaptive Life-History Trait Dependent upon Cuticular Hydrocarbons, and Influenced by Mating Status and Temperature in *D. Melanogaster*. *J. Insect Physiol.* **2020**, *121*, 103990. <https://doi.org/https://doi.org/10.1016/j.jinsphys.2019.103990>.

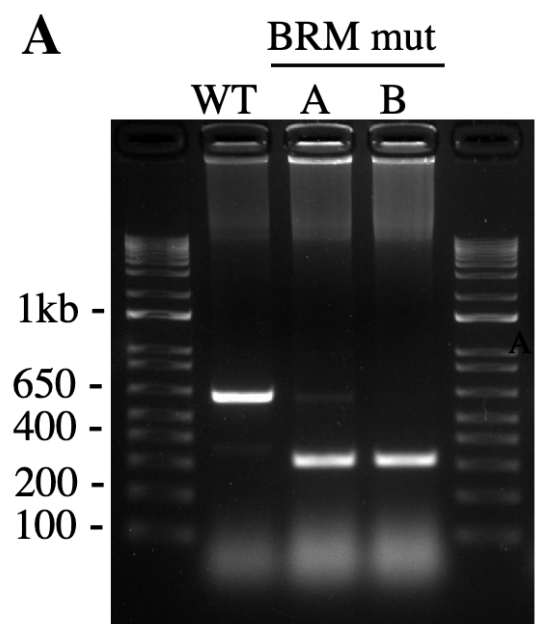
11:00 am

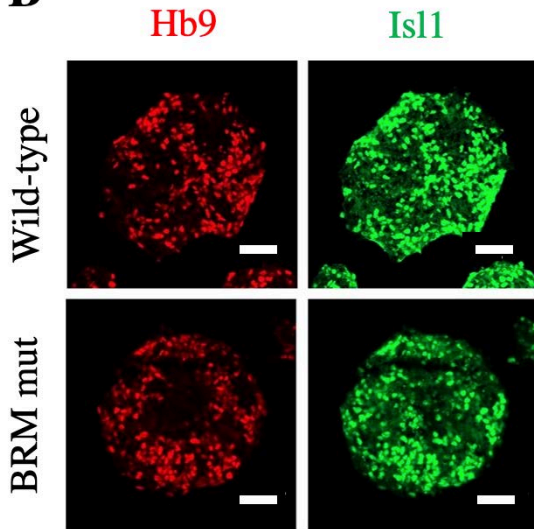
Alyssa Ialongo (Ho Sung Rhee)

Understanding the role of Neuronal BRG-1 Associated Factor (nBAF) protein during spinal motor neuron differentiation

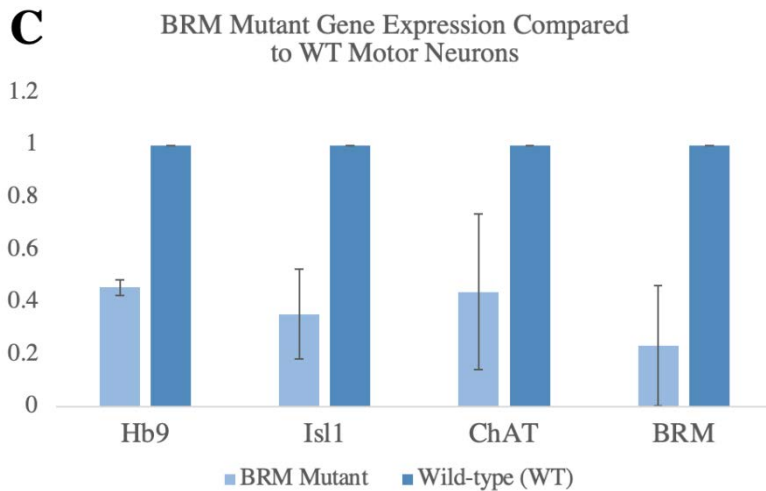
Chromatin remodelling is a critical process that occurs when embryonic stem (ES) cells differentiate into spinal motor neurons (MNs). One complex responsible for this process is Neuronal BRG1/BRM-Associated Factor (nBAF). nBAF is an ATP-dependant chromatin remodelling complex expressed in maturing MNs. nBAF is responsible for regulating the expression of genes necessary for proper dendritic morphogenesis and outgrowth in post-mitotic neurons by making their regulatory DNA regions accessible for transcription machinery. Recent studies suggest an important developmental role of the nBAF complex as mutations in this complex often have severe developmental impacts causing disorders such as developmental and epileptic encephalopathies, Coffin-Siris Syndrome, Nicolaides-Baraitser syndrome, schizophrenia, and autism. Although some functions of nBAF have been studied, how expression of important neuronal genes are changed by nBAF is unknown. To study this, each stage of differentiation was compared between wild-type and BRM mutants, which is a key protein within the nBAF complex. It was hypothesized that stages prior to mitotic cell cycle exit would be unaffected, but those thereafter will be affected in BRM mutants, and exhibit decreased expression of important neuronal genes. To study this, a 310 base-pair frameshift deletion in the exon 3 of BRM ES cells was confirmed using gel electrophoresis and sequencing. As expected, the pluripotency and ability to differentiate was not affected in the mutant ES cells based on alkaline phosphatase assay results. However, based on immunostaining and RT-qPCR results, the expression of important neuronal genes such as Hb9, Isl1 and ChAT in post-mitotic motor neurons was decreased 54-65% compared to wild-type MNs. These results indicate that the nBAF complex is important for the proper expression of neuronal genes such as Hb9, Isl1 and ChAT in post-mitotic spinal MNs.

**Figure A.** Genotyping of mouse ES cells containing BRM mutations. Agarose gel electrophoresis image of PCR products for WT ES cells exon 3 in column 2 (635bp) and BRM mutants with 310bp deletion in exon 3 in columns 3 and 4 (325bp).



**B**

**Figure B.** Wild-type and BRM mutant ES cells were differentiated into motor neurons. Confocal microscopy images taken at 20x magnification of day 6 wild-type (WT) embryoid bodies (top) and BRM mutant embryoid bodies (bottom) stained for important neuronal genes Hb9 and Isl1. White scale bar indicates 50μm.

**C**

**Figure C.** Downregulation of neuronal genes in BRM mutant cells compared to wild-type cells. RT-qPCR results showing wild-type (WT) and BRM mutant day 6 motor neuron gene expression levels. RT-qPCR was used to quantify the downregulation of important neuronal genes of such as Hb9, Isl1, ChAT, and BRM seen using confocal imaging.

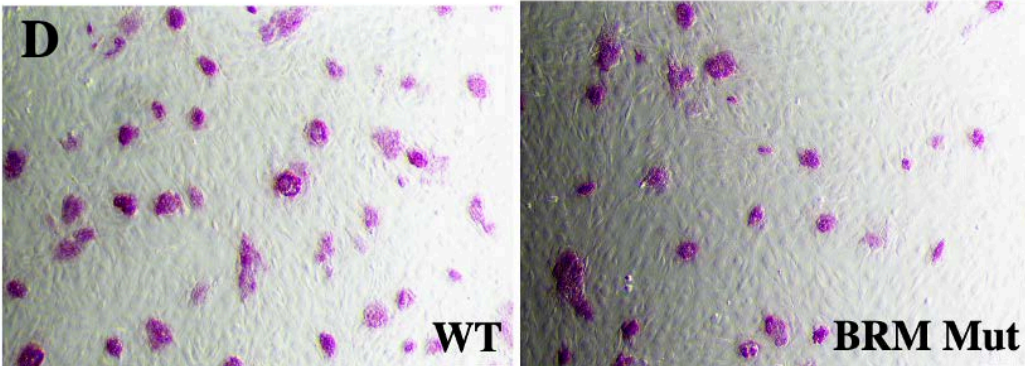


**Figure D.** Alkaline phosphatase assay of wild-type (WT) and BRM mutant cells. Light microscope images taken at 40x magnification of ES cells. Purple stain from alkaline phosphatase assay indicates pluripotency in both wild-type (WT) and BRM mutant ES cells.

11:15 am

Sarah De Costa (Tim Westwood)

### Spatially and temporally characterizing the Ecdysone response during *Drosophila melanogaster* embryogenesis

One of the most well documented hormones involved in insect development is 20-hydroxy ecdysone which is most known for its roles in metamorphosis, moulting, and eye development. The development of *Drosophila melanogaster* can be divided into several stages: embryogenesis; larval (three different instars), prepupal, pupal, and adult. Within each stage, ecdysone is found at varying concentrations and is the primary hormone responsible for triggering the events leading to progression into the next *Drosophila* life stage. This research aims to spatially and temporally identify ecdysone-regulated gene activity during embryogenesis. This was conducted in two parts. The first was to construct a prediction model of ecdysone responsive tissues in the embryo from publicly available RNA-seq transcriptome datasets. This prediction model provides information on the probability of finding a gene at a particular time and location to determine genes whose transcription is affected by ecdysone. In the second part, to verify the accuracy of these predictions, *in situ* hybridization experiments were performed using probes against a few of these ecdysone responsive genes to confirm their spatial and temporal RNA expression patterns. This study aims to create a comprehensive model to predict ecdysone-regulated gene expression during embryogenesis and the methods employed should be applicable to other biological processes that have similar types of RNA-seq data available.



**Figure 1.** Spatial and temporal localization of gene EIP75 during *Drosophila melanogaster* embryogenesis. Gene expression is localized in the midgut between stages 13-16. This image was obtained from the BDGP resource which conducted *in situ* hybridization on *Drosophila* embryos to track RNA expression.

11:30 am

Maria Roussi (Tim Westwood)

### Ecdysone mediated gene regulation throughout *Drosophila melanogaster* embryogenesis

20-Hydroxy ecdysone is a developmental steroid hormone that dictates several major life transitions during an insect's development. Studies have shown that ecdysone plays an important role in metamorphosis, molting, as well as in the development of insect's nervous system and eyes. This hormone has the ability to influence the expression of many genes that are collectively known as the Ecdysone Responsive Genes (ERGs). This research focuses on identifying ERGs and further analyzing ecdysone mediated gene regulation during *Drosophila melanogaster* embryogenesis. This was achieved by analyzing publicly available RNA sequence (RNA-seq) data using several computation methodologies. Upon ERG identification, clusters of genes were created utilizing R studio. These were further analyzed with Gene ontology (GO) programs. Clusters of induced and repressed genes were identified and further classified. The first classification emphasized the localization of gene expression in the developing embryo, while the second focused on their temporal expression profiles. If genes are localized in the same area and/or expressed at similar times, then it is more likely that these are regulated by similar factors. For detecting if and how

gene promoter regions are similar, and whether gene regulation was achieved by similar proteins, filtered and clustered genes had undergone motif enrichment analysis (MEA).

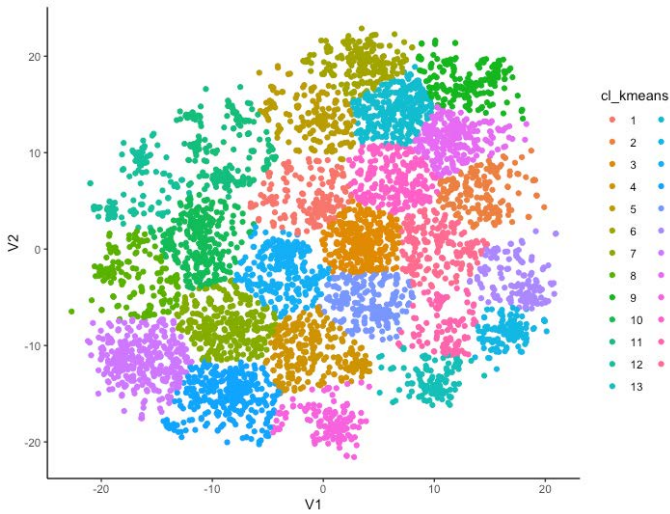


Figure 1: tSNE plot illustrating Kmean clustering with 25 clusters of genes been generated on R studio. Genes were clustered based on their expression in different cell types in different ecdysone concentrations, with a dispersion cut off value(P adj) of 0.05 and a log2FoldChange(FC) of 0.58 .

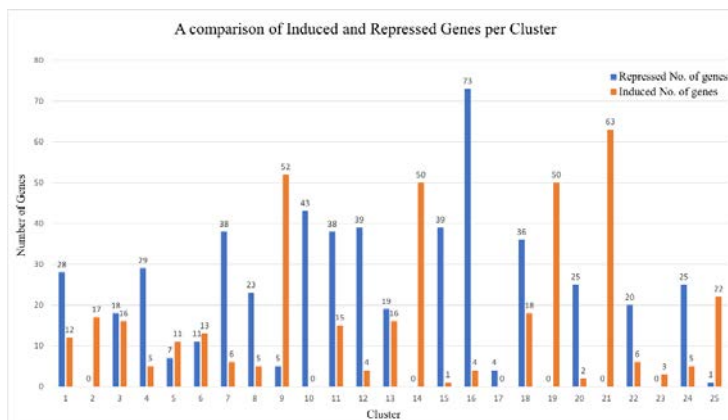


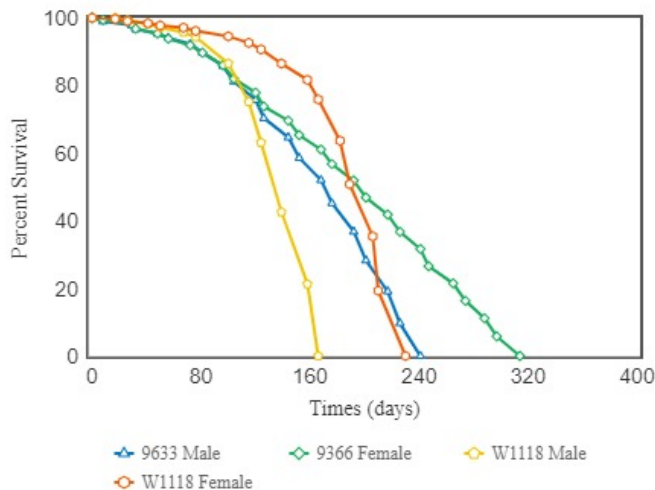
Figure 2: Bar plot comparing the number of significant Ecdysone Induced genes (396 in total) and Ecdysone Repressed genes (521 in total) in each cluster.

11:45 am

Erla Hidi (Tim Westwood)

### The Effect of the Proteasome-Associated Deubiquitinase USP14 on Proteasome Activity

Aging is thought to be associated with loss of function of many cellular and physiological mechanisms as well as general wear and tear of various cell macromolecules. One notable effect of aging is the accumulation of misfolded or damaged proteins within the cell. The Ubiquitin Proteasome Pathway plays an important role in combating this protein accumulation through selective protein degradation. This degradation is done through two general steps. First, the protein substrate which has been targeted for degradation is tagged by various enzymes working in succession and results in the addition of the short polypeptide ubiquitin (ub). The second step is where the 26S proteasome complex removes the ub tag from the substrate via deubiquitinases (DUBs) and degrades the target protein. In our model organism, *Drosophila*, our lab has previously found that when DUBs are reduced in the organism, the survivability (i.e. lifespan) under normal and stress conditions was increased (Fig.1). In this study, we aim to measure the rate of proteasome activity in several DUB deficient lines including ones deficient in USP14. We hypothesize that the proteasome activity will be increased in these lines compared to wild type resulting in better clearance of misfolded proteins and increased lifespan. In addition, we will be re-analyzing previously collected



survival data from the DUB deficient lines and other related deficiency lines. Our findings will provide some insight as to why reducing DUB levels results in increased lifespan.

**Fig.1** Line 9633 and W1118 death curve comparison. The figure above contains a visualization of the death curve data from USP14 deficient line 9633 and the wildtype line (W1118) for both sexes. Data was computed and visualized through OASIS2 using the non-parametric Kaplan-Meier analysis. Graph is taken from Vijayasathy (2020).

12:00 pm

John Stone (Tim Westwood)

Proteasome associated DUB USP14's effect of cellular proteasomal protein degradation activity

The interaction between aging, stress and cellular proteotoxicity is an important research line leading to greater understanding of aging at the cellular level, and with it, new abilities to medically treat age associated disease. The Ubiquitin proteasome pathway is a cellular mechanism for clearing excess improperly folded or otherwise damaged proteins and is essential for preventing cellular accumulation of proteotoxic stress. Deubiquitinating enzymes are associated with the proteasome complex and serve a regulatory function removing ubiquitin tags from proteasome degraded proteins, they also modulate proteasome efficiency. Genetic screens in the Westwood lab have shown that aneuploid mediated knockout of three DUBs: RPN11, USP14, and UCH37 has been associated with improved longevity in drosophila, both under normal conditions, and importantly under cellular stress conditions as well. Up to this point, the mechanism for this improved longevity and stress resistance was suspected to have been improved proteasome catalytic rate, as the DUBs were thought to be involved in a rate limiting step in proteasomal protein degradation. However, no data linking DUB knockout to improved proteasomal degradation rate has been generated. Here we presume to show, for the first time, that proteasome activity rates in drosophila melanogaster are directly increased by knockout of the DUB RPN11. We crossed fly stocks from RPN11 aneuploid lines with wildtype lines, and will perform activity assays on fly proteome samples to show that knockout of RPN11 is associated with increased proteasome catalytic rate, and we will also perform data analysis on past work to further strengthen the conclusion that this dub knockout is associated with longevity and cellular stress tolerance.

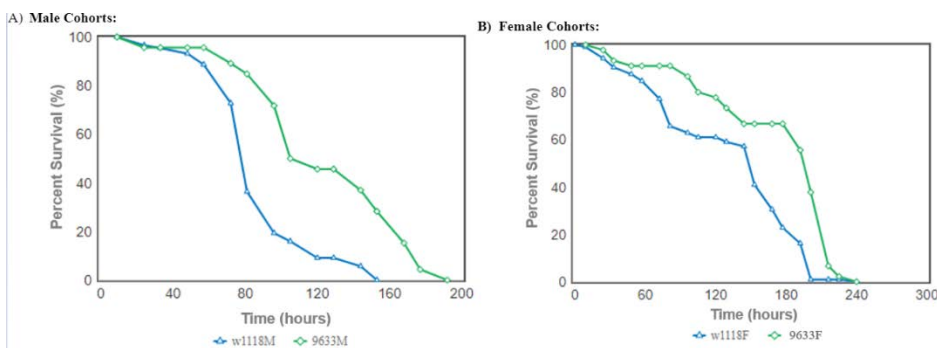


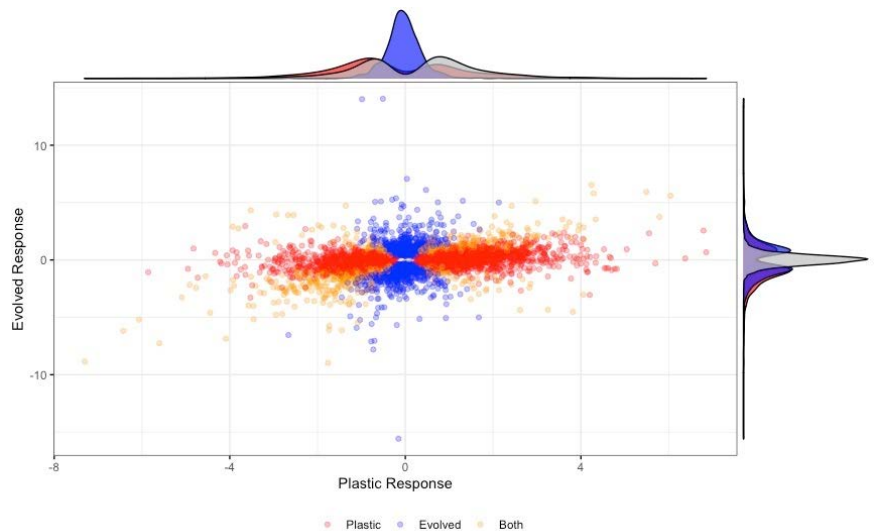
Figure 3: Kaplan-Meier survivorship curves for male (A) and female (B) cohorts of USP knockout line 9633 compared to control w1118 under chronic heat stress (32.8°C) over a 10-day period. Average lifespan of male 9633M (n=46) and female 9633F (n=45) are significantly greater than the average lifespan of control male w1118 (n=88) and female w1118 flies (n=105) (Gehan-Brewslow-Wilcoxon test,  $p < 0.05$ ). Source: Rai, Jayant. Investigating the Role of Deubiquitinase Enzymes on Drosophila Aging and Stress Fitness, Westwood Lab, (2013)

1:00 pm

Yeshoda Harry-Paul (Rob Ness)

### Methods of salt adaptation in *Chlamydomonas reinhardtii*

With the widespread use of road salt, pesticides, fertilizer, and other chemicals in our environment, salt is becoming a growing environmental concern. High salt levels in soil and aquatic settings impose major stress on organisms including animals, plants and the microbiome. The potential stress that salt can present is highlighted by the transition of very few aquatic species between salt and freshwater habitats. While the effects of salt pollution on ecology and physiology are currently the focus of much research, it is unclear whether the organisms evolve to meet the challenge. My project aims to identify the genes that allow this adaptation to occur. Using the model organism *Chlamydomonas reinhardtii*, cell lines were evolved to grow in increasing concentrations of salt until adaptation occurred to 36g/L NaCl. Gene expression levels were compared between ancestral cell lines and the adapted lines in both saline and control environments. Expression change was classified into four groups: genes with plastic expression between environments, ancestrally plastic genes fixed in evolved lines, genes that evolve plasticity and those with altogether new plasticity. These categories were functionally annotated and cross-referenced with the co-expression network to better understand them. Our results indicated that the most common form of adaptation was the evolution of entirely new gene expression. Genes displaying plastic responses to adaptation corresponded to genes relating to the cell membrane, while those displaying an evolutionary response (i.e. fixed, new plasticity and new expression groups), were related to nuclear assembly, ribosomes, protein phosphorylation, and photosynthesis.



1:15 pm

Wen Tong (Alex Nguyen Ba & Rob Ness)

### Determining the genetic basis of gene expression differences using scRNA-seq

A major goal of biology is understanding the molecular basis of phenotypes. Genetic mutations causing systematic variation in gene expression have been hypothesized as the one of the most important cause of phenotypic differences between individuals. However, studying the genetic basis of regulatory differences has traditionally been very laborious, requiring hundreds or thousands of full transcriptomes with corresponding genotypes. Here, we take advantage of advances in single-cell RNA sequencing (scRNA-seq) technologies to test whether this strategy is a viable technique for expression quantitative trait loci mapping (eQTL mapping). In contrast to typical scRNA-seq experiments that aims at identifying cell-types or cells from different species, we test whether we can simultaneously genotype and obtain whole-transcriptomes from single-cells of a population of *S. cerevisiae* from a meiotic cross. By comparing observed single nucleotide polymorphisms in transcripts to known genotypes in the pool of segregants, we successfully identified the genomes and transcriptomes of 13517 single-cells with an expected 5% error rate, out of 17510 single-cells sequenced. This represents a total 2915 possible unique genotypes out of 4489 individuals in the

pool. Thus, scRNA-seq may expedite the study of expression QTLs by simultaneously genotyping and phenotyping thousands of cells in a single experiment.

Figure 1

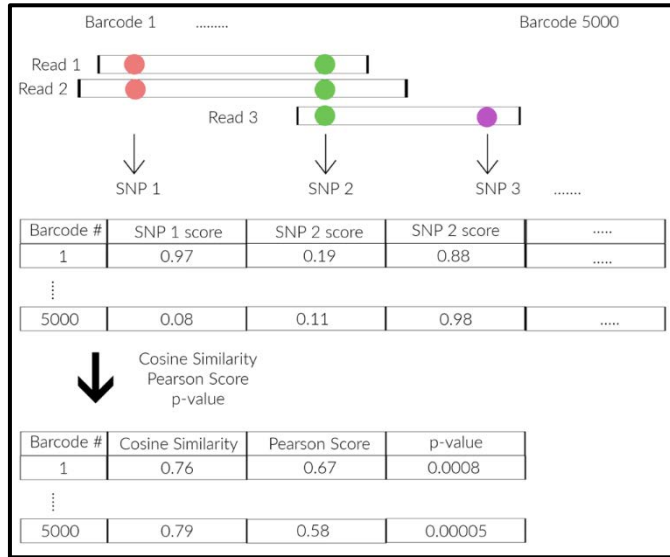


Figure 2

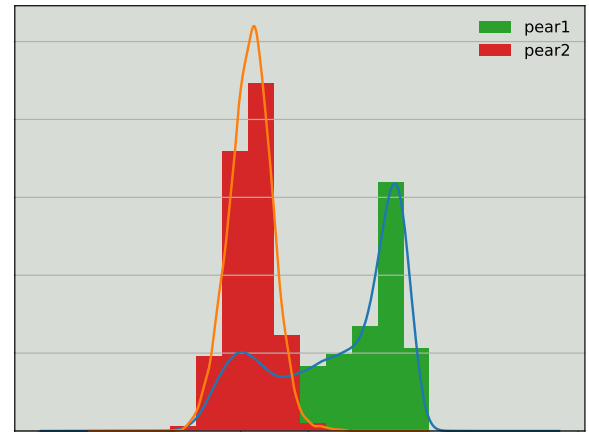


Figure 1: Method of identifying barcodes to *S. cerevisiae* haploid meiotic segregants cells

Figure 2: Best and second-best Pearson score of identity candidates for barcodes

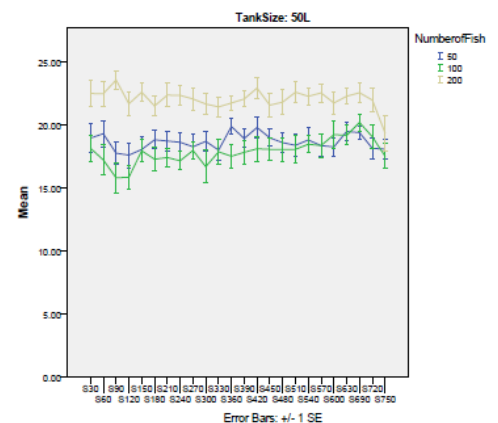
1:30 pm

Stephanie Shishis (Robert Gerlai)

## The Effect of Housing Density and Tank Size on the Behaviour of Adult Zebrafish: A Systemic Analysis

The zebrafish (*Danio rerio*) has become a staple in several fields of biology due to its evolutionarily conserved features leading to translational relevance coupled with its simplicity and ease of maintenance. Zebrafish are kept in a large number of laboratories around the world. Surprisingly, however, there is little known about what constitutes an optimal housing environment for these fish in the laboratory, with no systematic analysis performed to date. Recent literature has already begun to suggest that the current method of housing zebrafish in large numbers in small tanks is suboptimal, negatively impacting a plethora of biological phenotypes. Thus, in this study, we conducted the first systematic analysis on the potential impacts of housing density and tank volume on the welfare of zebrafish. Using a between subject design, we examined the behavioral effects of housing adult zebrafish in one of three tank sizes (1.5L, 10L, and 50L) with one of three housing densities (1, 2, and 4 fish/L) for 2 weeks. We found significant and behavior specific effects of the employed conditions. For example, we found bottom dwelling, immobility, intra-individual temporal variance of velocity, absolute turn angle and intra-individual temporal variance of turn angle to be affected by the above housing conditions, changes that likely reflect alterations in anxiety. The results suggest that both tank size and housing density may exert some negative, anxiety/stress inducing effects on behaviour, and thus should be considered in zebrafish maintenance.

Figure 1: Cumulative duration of immobility in the 50 L tank depends upon the number of fish housed in the tank.



1:45 pm

Joshua Hung (Marcus Dillon)

### Pangenome Analysis of *Xanthomonas* Outbreaks

The *Xanthomonas* genus includes more than 25 species that cause disease in a wide range of plant hosts, including essential crops like rice and tomatoes. This diversity of host species provides an excellent model for us to study the genomic features that govern host specificity with comparative genomics. Using a bioinformatics pipeline, we developed a pangenome profile for a diverse array of 58 *Xanthomonas* strains, all of which have been whole-genome sequenced. These strains represent 16 canonical *Xanthomonas* species, were isolated from 28 hosts, and originate from 25 countries. Quality control was first performed on each assembly using QUAST and BLAST, which caused us to abandon one assembly. The remaining 57 genomes were then annotated using PROKKA and a pangenome profile for the genus was constructed using PIRATE. The *Xanthomonas* pangenome consists of 14,299 gene families across these 57 constituent genomes, with 1,289 and 2,057 families being present in the hard (100% threshold) and soft (95% threshold)-core pangenomes, respectively. The small core-genome indicates that only a small number of essential genes are required across *Xanthomonas* isolates that are derived from different hosts. Finally, using established alignment algorithms and phylogenetic analysis, we show that strains isolated from the same host and even some strains that have been assigned the same species designation do not constitute monophyletic groups. This suggests that multiple lineages of *Xanthomonas* have converged to cause disease on the same hosts and may allow us to highlight the specific pathways that govern these adaptations in future genome-wide association analyses.



2:00 pm

Marian Saab (Melissa Holmes)

### Valproic Acid Alters Social Behaviour in Naked Mole-rats (*Heterocephalus glaber*)

Naked mole-rats are eusocial rodents that live in hierarchical colonies with distinct behavioural roles. In other eusocial animals, pharmacologically-induced epigenetic modifications produce sustained alterations in gene expression, which can cause deviations in the behaviour and ascribed roles of individuals within the colony. The present study explored the effects of valproic acid (VPA), a histone deacetylase inhibitor, on the social behaviour of naked mole-rats. Adult subordinate animals underwent twice daily peripheral injections of VPA or saline for one week, after which they were paired with an unfamiliar conspecific of the opposite sex. Additionally, we performed protein assays to assess alterations in histone acetylation within the brain and changes in pheromonal protein

composition in the urine. We found that female stimulus animals paired with VPA-treated males exhibited increased genital, body, and face investigation. In contrast, female experimental animals displayed changes in genital investigation towards a stimulus animal. Preliminary results from the protein assays show an increased histone modification on H3K18 among VPA-treated males and a presence of major urinary proteins in animals only after exposure to unfamiliar conspecifics. Overall, VPA may facilitate the transition of sexual maturity in female animals through direct administration or mediation by an opposite-sex individual that received the drug, suggesting either the brain or liver influences individual differences that mediate social phenotype in the colony.

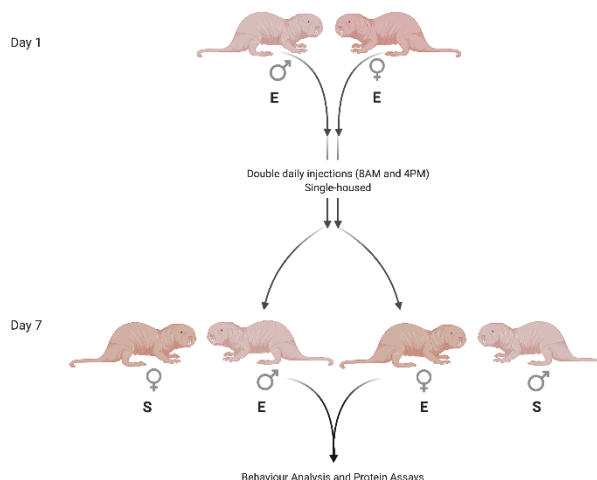


**Fig 1. Experimental Workflow.** Adult experimental (E) naked mole-rats underwent double daily peripheral injections of Valproic acid or saline for one week, and were subsequently paired with an unfamiliar stimulus (S) conspecific of the opposite sex. After tissue collection, a Western blot was performed on brain tissue to assess histone acetylation, and a Coomassie protein stain was used to characterize pheromonal protein composition in urine. Behavior analysis was then performed to investigate changes in behavior after exposure to stimulus animals.

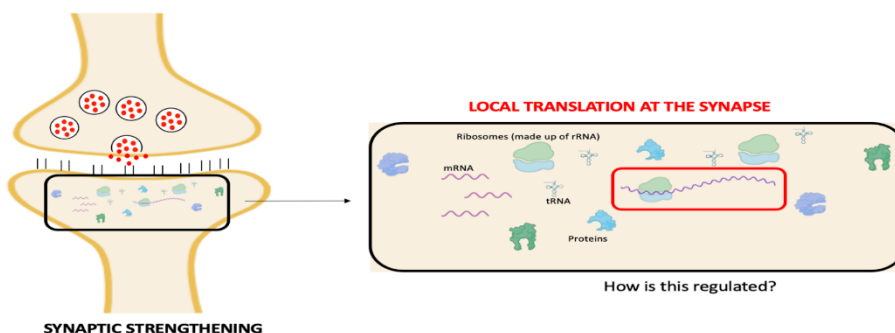
Created with BioRender.com

2:15 pm

Fiona Ramnaraigh (Brandon Walters)

### Characterizing the Diversity of RNA Modifications Localized at the Hippocampal Synapse

Memory formation is thought to occur through the strengthening and weakening of synapses, selectively involved in each learning event. While prior studies have shown the transcriptional basis of synaptic changes, contributions by translation are poorly understood. In neurons, translation occupies a unique role, as outpost ribosomes exist locally in synapses, allowing local translation to occur specifically within the synapse.



It is currently not clear how local synaptic translation is regulated, but RNA modifications have been shown to regulate translation globally, providing a potential mechanism for this regulation. However, RNA modifications are numerous, and uncharacterized, with less than 1% of RNA modifications being extensively studied, and nothing is known about their distribution within neurons. In this study, we identify RNA modifications contained both within the hippocampus, as well as those present specifically within synapses. We isolated RNA from the different subcellular compartments of neurons and analyzed the composition of nucleic acids by mass spectrometry. The results of this study will provide essential insight into the role of RNA modifications in the brain, by revealing if RNA modifications are present, but also if they show any preference for synaptic localization, suggesting a potential regulatory mechanism of local translation within synapses.



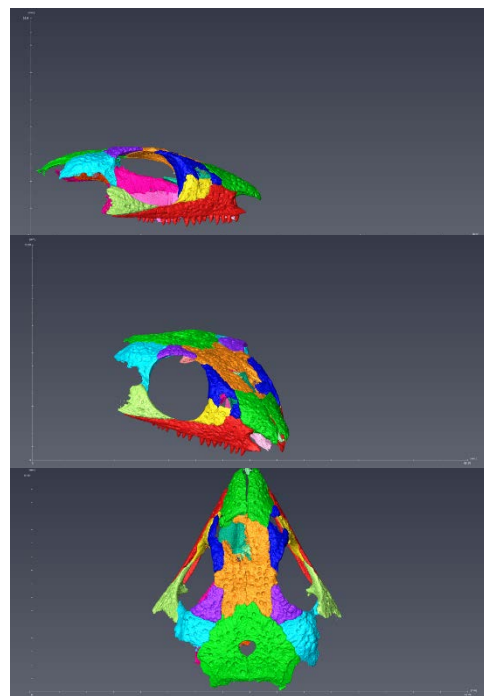
attempted. Here, evidence of entities resembling Giant viruses and PLVs in *C.parva* viral lysates is shown. TEM negative staining images of concentrated CpV lysates revealed two reoccurring icosahedral particles within the sample, with diameters of ~250nm and ~50nm. Attempts of isolating distinct CpV morphologies using lodixanol density gradients were inhibited by bacterial and host-cell contaminant aggregation. This study serves as a starting point for isolation of CpVs and associated virophages to deeper understand virus-virophage-host dynamics.

3:00 pm

Erin Beaudesne (Robert Reisz)

### A New Early-Permian Parareptile from Richards Spur, Oklahoma

A tiny partial skull obtained from the Dolese Brothers limestone quarry near Richards Spur, Oklahoma provides evidence for a new genus of parareptile which was alive during the Lower Permian (289 Ma.) in this area. The newly discovered specimen includes an articulated, nearly complete skull roof and several palatal bones, including the left pterygoid, epipterygoid, palatine and vomer. Through detailed comparisons of this skull to those of contemporary parareptiles *Acleistorhinus pteroticus*, *Delorhynchus cifellii* and *Colobomycter pholeter* it can be determined that this new specimen likely represents a new genus of acleistorhinid and is most similar to *Acleistorhinus pteroticus* in terms of morphology. Because of how similar this specimen is to *Acleistorhinus pteroticus*, this paper will focus on pointing out the differences between these two distinct taxa of parareptiles. Unique aspects of the present specimen, such as the pronounced anterior extension of the lacrimal bone, homodont dentition, increased fields of the palatal dentition and the location of the pineal foramen will be discussed in depth. The discovery of this new parareptile along with the staggering number of others discovered at Richards Spur highlights the importance of the unique fissure and vertical cave system at this site which has allowed for the preservation of articulated materials. No other site has provided such a wide diversity of parareptile taxa, part of a complex community of terrestrial vertebrates. The present specimen will certainly not be the last new species discovered at this astonishing site.



Exploring seasonal variation of methylmercury in lake trout (*Salvelinus namaycush*)

Methylmercury (MeHg) is a neurotoxic organic contaminant. By accumulating in proteinaceous tissues, MeHg biomagnifies in aquatic food webs and reaches its greatest concentrations in high trophic level organisms like fishes. Consequently, MeHg contamination may pose serious health risks to both aquatic organisms themselves and to the humans who consume them. Currently, little is known about how MeHg exposure or elimination varies on a seasonal basis and what factors may drive these patterns. Here, we aimed to identify seasonal MeHg trends in the top predator sport fish, lake trout (*Salvelinus namaycush*). Lake trout undergo seasonal dietary shifts which may generate seasonality in MeHg exposure over the course of the year. To test this, lake trout were sampled seasonally across two years between 2017 and 2019 in two lakes located within Algonquin Park: Lake Opeongo (OPE) and Lake of Two Rivers (LTR). These lakes have different community structures that shape lake trout diet. To capture seasonal trends, we measured total mercury content (THg) and MeHg concentration in the liver of each fish (n=80 for LTR, n=83 for OPE). Using these values, we also calculated %MeHg ( $[\text{MeHg}]/[\text{THg}]$ ) for each liver to examine the interplay of MeHg exposure and elimination across seasons. Although we found no significant difference in MeHg concentration or %MeHg between lakes, we did identify significant differences in %MeHg in LTR when comparing this variable by season in the second year of sampling. Consequently, our results demonstrate that seasonality may be an important factor in understanding how MeHg cycles over time and thus should be explored further.

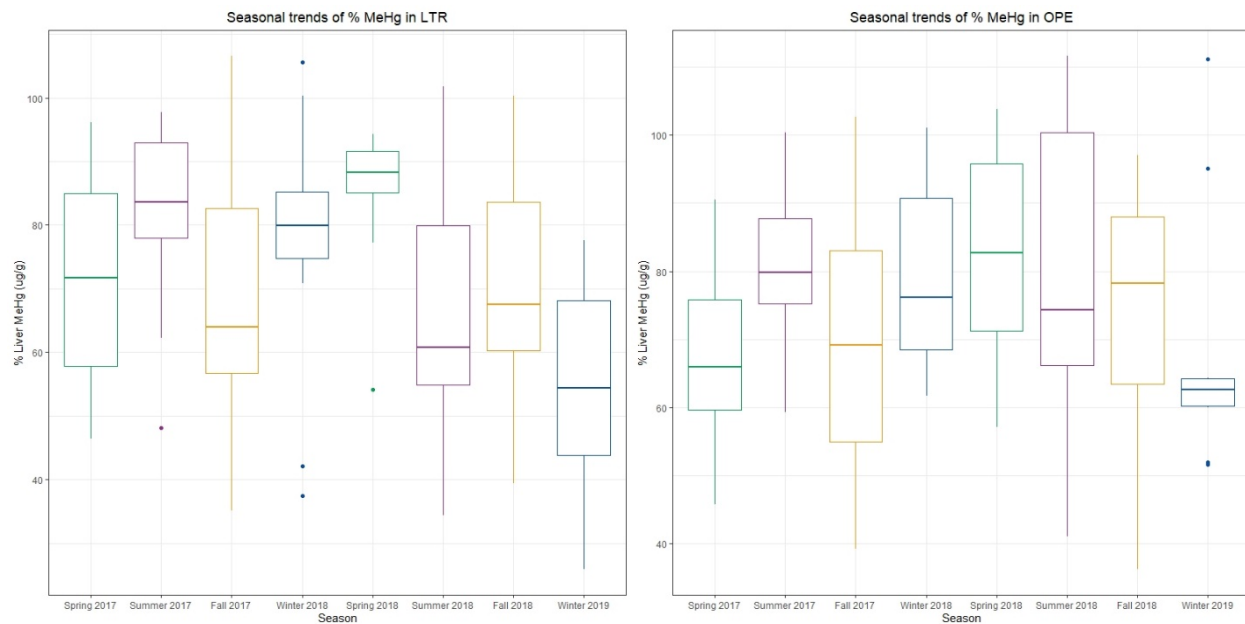
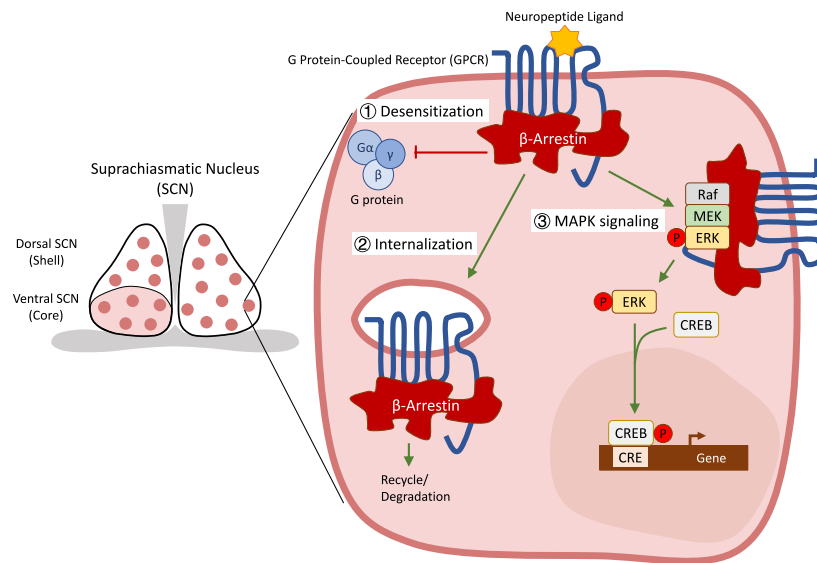


**Figure 1:** Side by side boxplots compare seasonal trends in % Liver MeHg [MeHg/THg] of lake trout (*Salvelinus namaycush*) sampled from Lake of Two Rivers (LTR, left) and Lake Opeongo (OPE, right).

The roles of  $\beta$ -arrestin 1 in the GPCR-regulated circadian rhythm pathways in mice

Neurons of the suprachiasmatic nucleus (SCN), the mammalian master circadian pacemaker, rely on G protein-coupled receptor (GPCR)-mediated signal transduction to adjust the phase of circadian rhythms based on environmental time cues.  $\beta$ -Arrestins are responsible for GPCR desensitization, internalization and downstream signaling in general, yet their mechanisms within the SCN remain obscure. This study reveals that  $\beta$ -arrestin 1 ( $\beta$ -arr1) modulates the activity of mitogen-activated protein kinases/extracellular signal-regulated kinases (MAPKs/ERKs) to control murine circadian rhythms and light-induced clock resetting. Mice lacking  $\beta$ -arr1 had damped behavioral rhythms. They were less responsive to photic cues: they did not entrain to light cycles efficiently and exhibited negligible light-induced phase shifts. At the cellular level, the rhythmic activation of ERK1/2 was damped and phase-delayed in the SCN of  $\beta$ -arr1 knockout mice. In the absence of  $\beta$ -arr1, we observed heightened activation of ERK in the SCN following a nocturnal light pulse. Collectively, these data suggest that  $\beta$ -arr1 is required for light-induced clock resetting and robust circadian behaviour by regulating MAPK/ERK activity downstream of GPCRs.



Collectively, these data suggest that  $\beta$ -arr1 is required for light-induced clock resetting and robust circadian behaviour by regulating MAPK/ERK activity downstream of GPCRs.

**Graphical Abstract:** The structure of mice SCN and three major functions of  $\beta$ -arr1 in the GPCR-mediated circadian

rhythm pathways in mice. 1)  $\beta$ -Arr1 desensitizes GPCR by steric inhibition of G protein; 2) GPCR-bound  $\beta$ -arr1 signals for the endocytosis of GPCR, which leads to GPCR recycling or degradation; 3)  $\beta$ -arr1 act as a scaffold for MAPK signaling, by which it recruits and activates Raf, MEK and ERK that further activates downstream transcription factors for relative gene expressions.

### The Effect of TCF12 Deficiency on Circadian Rhythm

Circadian rhythms allow adaptation of sleeping, feeding, and other behaviours in anticipation of external environmental cues such as the light-dark cycle. The molecular basis of circadian rhythms lies in a set of transcription-translation feedback loops (TTFLs) that drives the rhythmic transcription of core clock genes. Different genes are involved in governing circadian timekeeping via modulation of the core clock component, but many remain uncharacterized. In mammals, a bilateral structure in the anterior hypothalamus called the suprachiasmatic nucleus (SCN) is the principal pacemaker that coordinates circadian rhythms throughout the body via hormonal secretion and cell-to-cell interactions. Members of the TCF gene family encode basic helix-loop-helix (bHLH) transcription factors that recognize the consensus binding site, the E-box element. By using conditional knockout (cKO) mice deficient for TCF12 in the SCN, we investigated the role of TCF12 in the regulation of circadian rhythms. First, we confirmed the efficacy of the ablation using Western blot and immunohistochemistry to examine the expression of TCF12 in the SCN region. Then, we analyzed circadian wheel-running behaviour in TCF12 deficient mice and littermate control mice through phase shift and jet lag lighting schedules. By comparing TCF12 cKO mice and control mice, we found that there was no difference in circadian period under constant dark conditions or acute photic resetting. On the other hand, TCF12 cKO mice took significantly more days to re-entrain to jet lag paradigms. This result reveals that TCF12 is required for recovery for jetlag. The mechanisms for this phenotype remain unknown but could involve changes in the regulation of Period (Per) gene expression in the SCN.

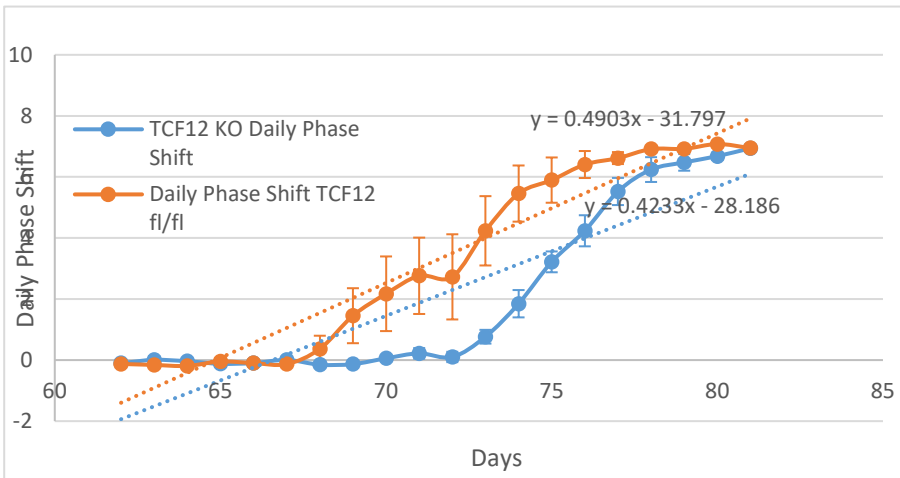


Figure 1.1 demonstrates TCF cKO mice and littermate control mice’s average daily phase shift changes from wheel-running behavioural analysis day 62 to day 81. TCF12 cKO mice take longer to re-retrain to jet lag paradigms since its linear regression line is less steep compared to the control mice. Stand error of mean is shown at each data point.



Figure 1.2 is the boxplot of the average phase shift under the acute photic resetting for both TCF12 cKO mice and the control mice. There is no significant difference between these two groups ( $p > 0.05$ ).

Optimizing the expression and secretion of Irisin in the probiotic yeast strain *Saccharomyces boulardii*

Inflammatory bowel disease (IBD), a chronic disorder that causes inflammation in the intestine, has few effective treatment options due to its location. While current options mostly depend on indirect administration of the drug, genetically engineered microbes may be used to address this issue, as the intestine is a natural environment for a large and diverse group of microbes. Advances in the field of synthetic biology have led to the discovery of numerous tools and techniques that allow us to re-purpose the internal environment of a cell. Using these tools, we can genetically engineer microbes into a probiotic that can deliver a therapeutic peptide directly at the site of inflammation. One potentially therapeutic peptide is called irisin – a hormone-like peptide derived from a cleaved product of the FNDC5 gene in mammals. This project attempts to genetically engineer a probiotic strain of yeast – *S. boulardii* – to express and secrete irisin within the intestine to alleviate symptoms of IBD. In combination with a 12X-His solubility tag, a galactose-inducible promoter called pGAL and a tGUO1 yeast terminator sequence was used to flank the irisin expression cassette in a yeast plasmid DNA construct. Plasmids and primers were designed and cloned with additional solubility tags from the UBI4 and TRX2 genes, as well as a high copy plasmid. Current progress has found an effective way to express irisin in *S. cerevisiae* models with the TRX2 solubility tag, and further experiments are being done to mimic and optimize this expression in *S. boulardii*.

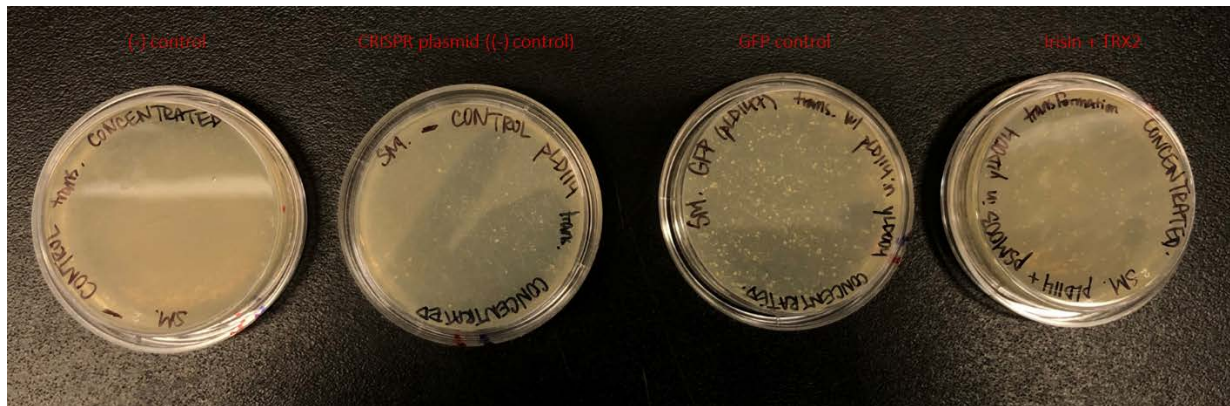


Figure 1: Results of genomic integration of genetically engineered irisin expression plasmid into *Saccharomyces boulardii*.

**Irisin Expression Cassette – TRX2**



Figure 2: Components of the genetically engineered irisin expression cassette for expression in *Saccharomyces cerevisiae*. This includes a yeast-specific promoter, two separate solubility tags, the Irisin gene, and a yeast terminator sequence.

Thank you to our judges:

- Prof. Sasa Stefanovic
- Prof. Adriano Senatore
- Prof. Katharina Breutigam
- Prof. Arbora Resulaj

Thank you to Prof. Peter Kotanen for teaching the course and moderating the sessions.

Thank you to all the supervisors for taking on these projects during an unprecedented time.

- Prof. Joel Levine
- Prof. Angela Lange
- Prof. Ted Erclik
- Prof. Ho Sung Rhee
- Prof. Tim Westwood
- Prof. Alex Nguyen Ba
- Prof. Bailey McMeans
- Prof. Mary Cheng
- Prof. Robert Gerlai
- Prof. Marcus Dillon
- Prof. Melissa Holmes
- Prof. Brandon Walters
- Prof. Steven Short
- Prof. Robert Reisz
- Prof. David McMillen